

# A Recipe for Efficient Sim-to-Real Transfer in Manipulation with Online Imitation–Pretrained World Models

Yilin Wang<sup>1†</sup>, Shangzhe Li<sup>2†</sup>, Haoyi Niu<sup>3</sup>, Zhiao Huang<sup>4</sup>, Weitong Zhang<sup>2</sup>, Hao Su<sup>1,4</sup>

**Abstract**—We are interested in solving the problem of imitation learning with a limited amount of real-world expert data. Existing offline imitation methods often struggle with poor data coverage and severe performance degradation. We propose a solution that leverages robot simulators to achieve online imitation learning. Our sim-to-real framework is based on world models and combines online imitation pretraining with offline finetuning. By leveraging online interactions, our approach alleviates the data coverage limitations of offline methods, leading to improved robustness and reduced performance degradation during finetuning. It also enhances generalization during domain transfer. Our empirical results demonstrate its effectiveness, improving success rates by at least 31.7% in sim-to-sim transfer and 23.3% in sim-to-real transfer over existing offline imitation learning baselines.

## I. INTRODUCTION

Training robotic policies in simulation or from offline datasets and then finetuning them in the real world is a common strategy for real-world robotic control [1], [2], [3], [4], [5], [6]. However, many of these works either require explicitly defined reward functions [2], [1], or depend on large-scale offline expert datasets [5], [6]. In contrast, we study a sim-to-real setting with limited expert demonstrations in both domains and no reward signals available.

This setting presents significant challenges for offline imitation learning [7], as limited expert coverage leads to overfitting and exacerbates bias accumulation; reinforcement learning approaches [8], [9], [10] are also inapplicable due to the absence of reward signals.

To address this, we propose a two-phase sim-to-real pipeline: (i) online imitation pretraining in simulation with simulated expert demonstrations and (ii) offline imitation finetuning with limited real-world demonstrations. During the pretraining phase, our method leverages a latent world model for efficient learning and employs the CDRED reward model [11] to generate reward signals by discriminating expert data from online interactions. Empirically, we show that online pretraining improves state-space coverage, reduces degradation after finetuning, and enhances out-of-distribution generalization. We further leverage a practical state estimation pipeline that fuses robot proprioceptive states with object pose

estimation, enabling real-world deployment. We evaluate our approach on six sim-to-sim transfer environments with two domain gaps and three sim-to-real transfer tasks. Our method achieves at least 31.7% success rate improvement in sim-to-sim transfer and 23.3% improvement in sim-to-real transfer over state-of-the-art offline imitation learning baselines.

Our main contributions are as follows: (i) Proposing an efficient sim-to-real framework for limited-data regimes via online imitation pretraining of world models. (ii) Demonstrating, through comparisons with offline imitation learning, that our method achieves superior out-of-distribution (OOD) generalization and is more robust to performance degradation after few-shot finetuning. (iii) Providing an empirical analysis that attributes these performance gains to the superior data coverage achieved during the online exploration phase.

## II. RELATED WORKS

*a) Online Imitation Learning:* Online imitation learning is a variant of imitation learning that leverages reward-free interactions with the environment to improve performance, particularly when the size of the expert dataset is limited. Generative Adversarial Imitation Learning (GAIL) [12] introduces a framework based on generative adversarial training to perform online imitation learning. Subsequent works [13], [14], [15] focus on stabilizing and improving GAIL within the adversarial imitation learning framework. Soft-Q Imitation Learning (SQL) [16] reformulates imitation learning as a reinforcement learning problem by assigning rewards of 1 to expert demonstrations and 0 to all other transitions. More recent approaches leverage model-based architectures to improve sample efficiency and performance, including standard model-based methods [17] and latent world model approaches [18], [19], [11].

*b) Sim-to-Real Transfer for Manipulation:* Sim-to-real transfer aims to deploy a robotics policy trained in simulation to the real world by addressing domain gaps between the two environments [20]. In robotic manipulation, prior works have explored a variety of approaches, including real-to-sim-to-real transfer with 3D reconstruction and point cloud-based policies [21], sim-to-real transfer for vision-based humanoid dexterous manipulation via a divide-and-conquer policy distillation framework [4], reinforcement learning-based transfer for deformable object manipulation [22], residual learning for efficient contact-rich manipulation [23], reinforcement learning methods for generalizable articulated object manipulation [2], vision-language model-generated rewards for real-to-sim-to-real transfer [24], and diverse synthetic data generation for sim-to-real reinforcement learning [25].

† Equal contributions.

<sup>1</sup>Yilin Wang and Hao Su are with the Department of Computer Science and Engineering, University of California, San Diego.

<sup>2</sup>Shangzhe Li is with the Department of Computer Science, and Weitong Zhang is with the School of Data Science and Society, University of North Carolina at Chapel Hill.

<sup>3</sup>Haoyi Niu is with the Department of Mechanical Engineering, University of California, Berkeley.

<sup>4</sup>Zhiao Huang and Hao Su are with Hillbot Inc.

Unlike existing reinforcement learning-based approaches, our method relies purely on imitation learning, eliminating the need for reward signals in both simulation and the real world. Furthermore, in contrast to offline imitation learning methods that use demonstration datasets only, our approach leverages online interactions in a simulator to achieve broader data coverage through active exploration.

### III. PRELIMINARY

#### A. Problem Formulation

We formulate our problem as a Markov Decision Process (MDP), defined by the tuple  $\langle \mathcal{S}, \mathcal{A}, \mathcal{P}, r, \gamma \rangle$ , where  $\mathcal{S}$  is the state space;  $\mathcal{A}$  is the action space;  $\mathcal{P} : \mathcal{S} \times \mathcal{A} \rightarrow \Delta_{\mathcal{S}}$  is the transition function;  $r : \mathcal{S} \times \mathcal{A} \rightarrow \{0, 1\}$  is a sparse reward function that encodes binary success or failure feedback—assigning a reward of 1 to the final state-action pair of a successful trajectory, and 0 otherwise.  $\gamma \in [0, 1]$  is the discount factor. Our goal is to learn a policy  $\pi : \mathcal{S} \rightarrow \Delta_{\mathcal{A}}$  that minimizes the statistical distance between the state-action distribution induced by the policy,  $\rho_{\pi}$ , and the expert distribution  $\rho_E$ , using a set of expert state-action transitions in the simulator. We then aim to transfer the learned policy  $\pi$  to the real world, where both the transition and reward function (unknown to the agent) may differ from those in the simulator.

#### B. World Models

In our setting, *world model* is referring to reinforcement learning or imitation learning methods that explicitly learn a data-driven approximation of the environment’s transition dynamics—commonly known as model-based approaches. A key line of recent progress in this area is the development of latent-space world models [26], [27], [28], [10], which employ an encoder  $\mathbf{z} = h(\mathbf{s})$  to map observations into a compact latent representation and a dynamics model  $\mathbf{z}' = d(\mathbf{z}, \mathbf{a})$  to predict transitions within that latent space. By predicting future latent states and generating imagined rollouts, these models enable efficient planning, leading to high sample efficiency and strong performance across a broad spectrum of challenging tasks [10].

### IV. METHODOLOGY

In this section, we introduce our sim-to-real framework designed for settings with **no rewards** and only **limited expert data** in both simulation and the real world.

#### A. Overview on the Setting

In prior works, it is commonly assumed that a reward function is available in both simulation and the real world for reinforcement learning training [2], or that a sufficiently large offline expert dataset is accessible for imitation learning [5]. In contrast, we consider a more challenging setting where no reward functions are defined in either simulation or the real world. Instead, we rely on two small reward-free datasets, one from the simulation and one from the real environment, each consisting of expert demonstrations used for imitation pretraining and finetuning, respectively. While interactions are

permitted in the simulation environment, real-world finetuning depends solely on the limited expert dataset collected in the real world.

#### B. Overview on the Method

The overall pipeline of our sim-to-real approach with a world model consists of three stages: online imitation pretraining in simulation, offline finetuning with real-world data, and real-world deployment. First, we pretrain the world model using CDRED reward model [11] to discriminate between expert data and online interactions in the simulated environment (Section IV-C), leveraging state-based observations and 1M reward-free interactions. Next, we finetune the learned policy and encoder networks with a small dataset of expert demonstrations from the real world using a supervised finetuning objective (Section IV-D). The full pretraining and finetuning pipeline is illustrated in Figure 1. Finally, by employing a state pre-processing pipeline that converts camera RGBD observations into real-time pose estimates, combined with proprioceptive feedback from the robot, we deploy our world model for real-world robotic control tasks (Section IV-E). The pipeline for state pre-processing in real deployment is shown in Figure 2.

#### C. World Model Online Imitation Pretraining

Since no explicit reward signals are available during pretraining, standard reinforcement learning approaches for world model training, such as TD-MPC2 [10] and DreamerV3 [29], cannot be directly applied. To overcome this limitation, we adopt an *online imitation learning* framework [19], [11], [30]. In particular, we use the CDRED world model [11], an imitation-based variant of TD-MPC2 that incorporates a reward model to align expert and behavioral distributions through a coupled distributional random expert distillation module.

*a) Model architecture:* The CDRED world model consists of five core components. An encoder first maps the input state  $\mathbf{s}_t$  to a latent representation,  $\mathbf{z}_t = h(\mathbf{s}_t)$ . This latent state is then used by a latent dynamics model to predict the next state,  $\mathbf{z}'_t = d(\mathbf{z}_t, \mathbf{a}_t)$ , and a CDRED reward model to predict the immediate reward,  $\hat{r}_t = R(\mathbf{z}_t, \mathbf{a}_t)$ . For decision-making, the model also learns a value function,  $\hat{q}_t = Q(\mathbf{z}_t, \mathbf{a}_t)$ , and a policy,  $\hat{\mathbf{a}}_t = \pi(\mathbf{z}_t)$ , both of which operate on this latent state.

*b) Reward model:* The CDRED reward model consists of three parts: (i) an expert predictor  $f_{\phi}$ , (ii) a behavioral predictor  $f_{\psi}$ , and (iii) an ensemble of  $K$  frozen target networks  $\{f_{\theta_k}\}_{k=0}^{K-1}$ . The predictor and target networks estimate the densities of the expert and behavioral state-action distributions. These estimates are then used for reward construction. Following CDRED [11], the reward is defined as:

$$R(\mathbf{z}_t, \mathbf{a}_t) = -\zeta b(\mathbf{z}_t, \mathbf{a}_t, f_{\phi}) + (1 - \zeta) b(\mathbf{z}_t, \mathbf{a}_t, f_{\psi}) \quad (1)$$

where  $\zeta$  is a tunable parameter balancing the expert distribution bonus (encouraging exploitation of expert data) and the behavioral distribution bonus (encouraging exploration).  $b(\cdot)$  denotes the bonus term, which approximates the negative

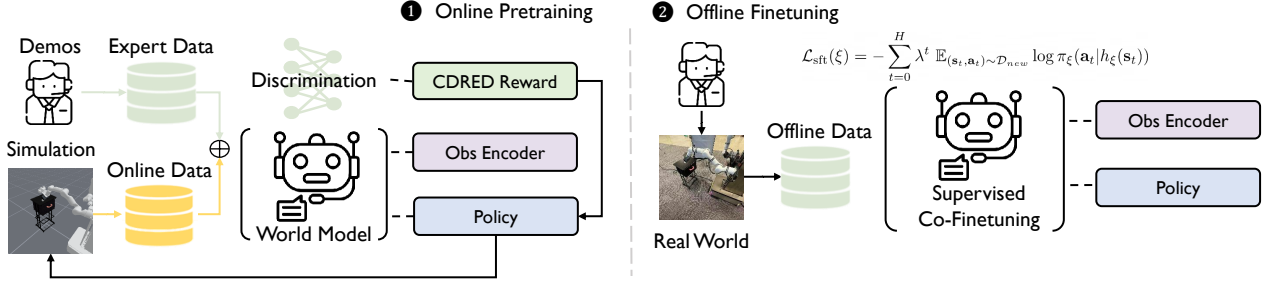


Fig. 1: **Sim-to-Real Pipeline with Online Imitation Pretraining.** We illustrate the pretraining and finetuning pipeline of our proposed method. During pretraining, the world model is trained using a reward signal from a jointly trained discriminator that distinguishes expert from online interaction data. In the finetuning phase, the pretrained encoder and policy are refined using a small dataset of real-world expert demonstrations.

log-likelihood with respect to a distribution (behavioral or expert). For example, if a datapoint  $(\mathbf{z}, \mathbf{a})$  lies within the distribution represented by  $f$ , then  $b(\mathbf{z}, \mathbf{a}, f)$  will be small.

c) *Training objective:* Given an expert buffer  $\mathcal{B}_E$  containing expert dataset  $\mathcal{D}$  and a behavioral buffer  $\mathcal{B}_\pi$  containing reward-free online rollouts, the world model is trained by minimizing:

$$\mathcal{L}(\phi, \psi, \xi) = \sum_{t=0}^H \mathbb{E}_{(\mathbf{s}_t, \mathbf{a}_t, \mathbf{s}'_t) \sim \mathcal{B}_E \cup \mathcal{B}_\pi} [\mathcal{L}^{\text{base}} + \mathcal{L}^{\text{reward}}(\phi, \psi)], \quad (2)$$

with the overall objective comprises two parts: a reward model loss  $\mathcal{L}^{\text{reward}}(\phi, \psi)$  and a joint loss  $\mathcal{L}^{\text{base}}(\xi)$  for training the encoder, dynamics, and Q-function:

$$\begin{aligned} \mathcal{L}^{\text{base}}(\xi) &= \lambda^t \left( \|\mathbf{z}'_t - \text{sg}(h_\xi(\mathbf{s}'_t))\|_2^2 + \text{CE}(\hat{q}_t, q_t) \right), \\ \mathcal{L}^{\text{reward}}(\phi, \psi) &= \lambda^t \mathbb{E}_{k \sim \text{Uniform}(0, K)} (T1 + T2), \end{aligned}$$

where  $\text{CE}$  denotes the cross-entropy loss, following [10], [11], for stabilizing critic learning, and  $\text{sg}$  denotes the stop-gradient operator. Here, the temporal difference target is computed with the CDRED reward:  $q_t = R(\mathbf{z}_t, \mathbf{a}_t) + \gamma Q(\mathbf{z}'_t, \pi(\mathbf{z}'_t))$ . The reward model objective is formulated as two MSE terms, analogous to the training objective of random network distillation [31], which estimate the densities of the expert and behavioral distributions for constructing the reward model:

$$\begin{aligned} T1 &= \mathbb{E}_{(\mathbf{s}_t, \mathbf{a}_t) \sim \mathcal{B}_E} \left[ \|\mathbf{f}_\phi(\mathbf{z}_t, \mathbf{a}_t) - \mathbf{f}_{\bar{\theta}_k}(\mathbf{z}_t, \mathbf{a}_t)\|_2^2 \right], \\ T2 &= \mathbb{E}_{(\mathbf{s}_t, \mathbf{a}_t) \sim \mathcal{B}_\pi} \left[ \|\mathbf{f}_\psi(\mathbf{z}_t, \mathbf{a}_t) - \mathbf{f}_{\bar{\theta}_k}(\mathbf{z}_t, \mathbf{a}_t)\|_2^2 \right]. \end{aligned}$$

d) *Policy optimization:* A policy is then trained using the maximum-entropy objective similar to the one used in Soft Actor-Critic [8] but with a discounted summation over the horizon  $H$ :

$$\mathcal{L}^\pi(\xi) = \sum_{t=0}^H \lambda^t \mathbb{E} [-Q(\mathbf{z}_t, \pi_\xi(\mathbf{z}_t)) + \beta \log \pi_\xi(\cdot | \mathbf{z}_t)],$$

where the expectation is taken over all state-action pairs sampled from  $\mathcal{B}_E$  and  $\mathcal{B}_\pi$ . For training stability, we stop gradients from the policy learning objective from propagating into the encoder, following [10].

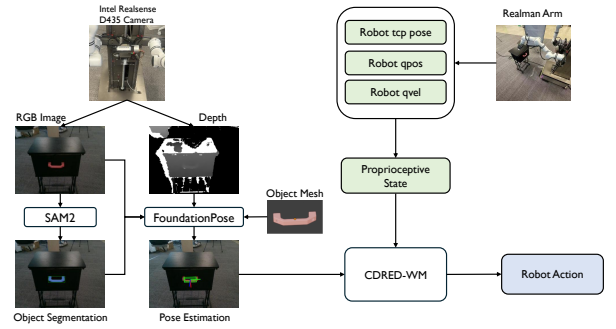


Fig. 2: **State Pre-processing during Real Deployment.** We illustrate the state pre-processing pipeline used during real-world deployment. The object pose is estimated from RGBD camera observations using SAM2 and FoundationPose. This estimate is then combined with the robot's proprioceptive states to form the input to the world model, which in turn generates actions for robotic control.

#### D. Offline Finetuning for Domain Transfer

After pretraining, we obtain a world model that performs well in the source domain. To transfer it to a new simulation domain or a real environment, we use a small expert dataset  $\mathcal{D}_{\text{new}}$  collected from the target environment for supervised finetuning. Specifically, we adapt both the encoder  $h_\xi$  and policy  $\pi_\xi$  by optimizing a maximum likelihood estimation objective over the horizon  $H$ :

$$\mathcal{L}_{\text{sf}}(\xi) = - \sum_{t=0}^H \lambda^t \mathbb{E}_{(\mathbf{s}_t, \mathbf{a}_t) \sim \mathcal{D}_{\text{new}}} \log \pi_\xi(\mathbf{a}_t | h_\xi(\mathbf{s}_t)). \quad (3)$$

Note that this finetuning is conducted fully offline, without any direct interaction with the new domain or the real environment. Instead, it only requires a small set of successful trajectories, which can be obtained, for example, through human teleoperation in the real world.

#### E. State Estimation in the Real World

The states for our model consist of 2 parts: robot proprioceptive states and object (such as cube or handle) poses. For the robot proprioceptive states, we directly get the qpos (arm

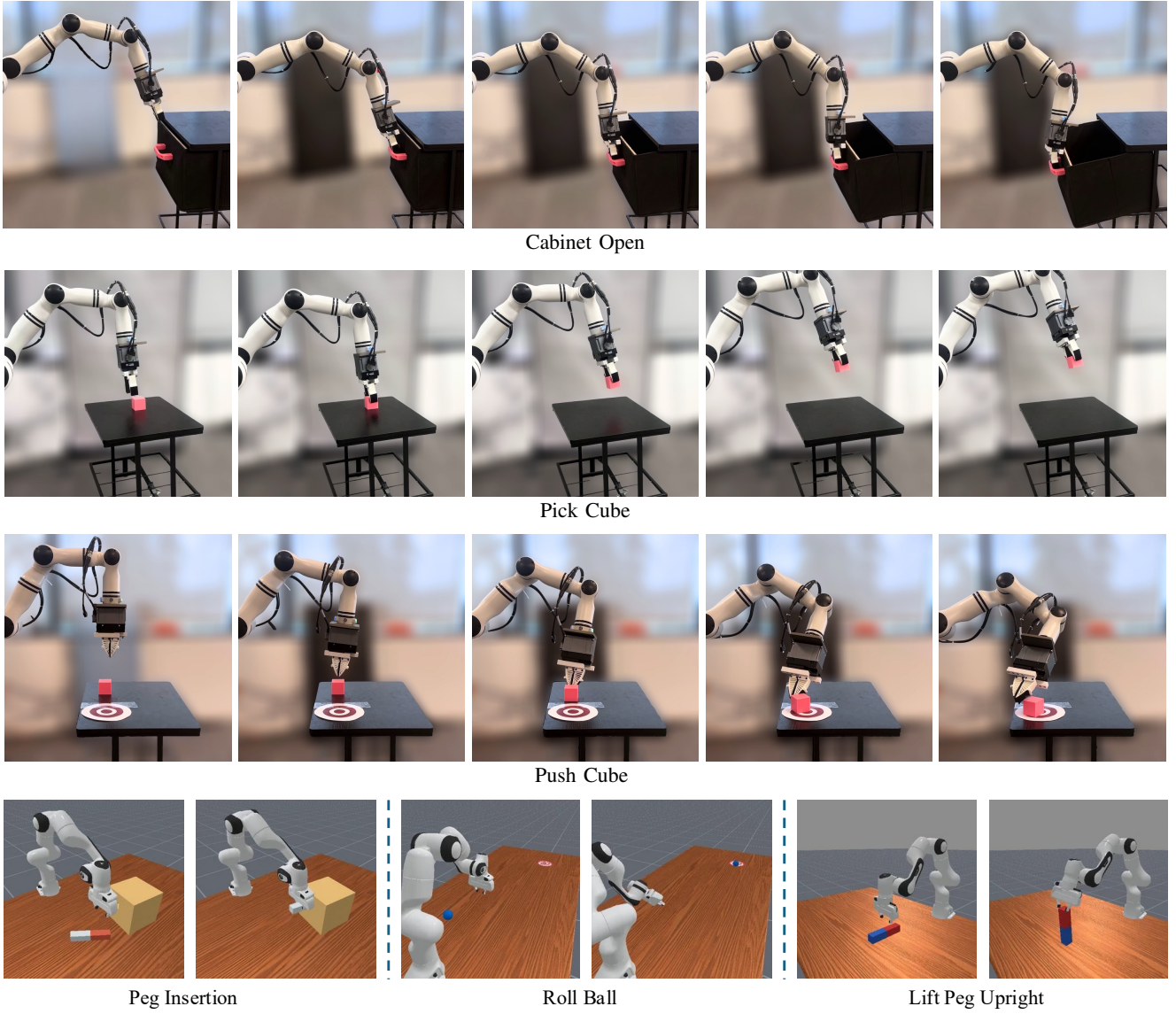


Fig. 3: **Illustrations of Tasks.** The first three rows show real-world demonstrations of the Cabinet Open, Pick Cube, and Push Cube tasks, while the last row presents the initial and final successful states of the Peg Insertion, Roll Ball, and Lift Peg Upright tasks in simulation.

and gripper joint values) from the robot, which can then be used to compute the qvel (arm and gripper joint velocity) and the pose of tcp (the link that connects the gripper with the robot arm).

For the object poses, an Intel RealSense D435 camera is used to estimate the object’s pose. First, the camera captures the RGB image and the depth map that contain the target object. Later, the RGB image goes through a SAM2 [32] model to get the object segmentation mask. The depth map, RGB image, segmentation mask as well as the object’s 3D mesh are then fed into a FoundationPose [33] model to estimate and track the object poses. These poses are then combined with the robot proprioceptive states and fed into our CDRED-WM model to get the actions for the robot during real-world deployment. The pipeline is illustrated in Figure 2.

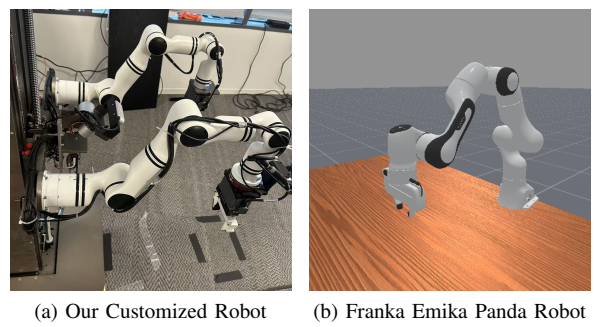


Fig. 4: **Illustration of Robots.** We show the two robot types used in our experiments: our customized robot and the Franka Panda. Since the Franka Panda arm is only used in simulation, we provide its simulated rendering, whereas for our customized robot we show real-world photo.

Tasks	Robot	Domain Gap	BC (Direct)	BC (P+F)	DP (Direct)	DP (P+F)	CDRED-WM (Ours)
Cabinet Open	Customized Robot	Biased Pose	18%	47%	8%	9%	<b>62%</b>
		Kinematics Gap	51%	51%	39%	36%	<b>66%</b>
		Biased Pose	16%	37%	34%	62%	<b>96%</b>
		Kinematics Gap	44%	73%	61%	73%	<b>83%</b>
		Biased Pose	35%	48%	90%	83%	<b>95%</b>
		Kinematics Gap	32%	29%	60%	71%	<b>72%</b>
Peg Insertion	Franka Panda	Biased Pose	8%	24%	0%	5%	<b>70%</b>
Roll Ball		Biased Pose	0%	4%	32%	35%	<b>47%</b>
Lift Peg Upright		Biased Pose	7%	58%	12%	25%	<b>93%</b>
Mean	-	-	23.4%	41.2%	37.3%	44.3%	<b>76.0%</b>

TABLE I: **Sim-to-Sim Transfer Results.** The results of sim-to-sim transfer experiments across various tasks with two types of domain gaps: biased pose and kinematics gap. BC refers to behavior cloning with an encoder and Gaussian policy, while DP denotes diffusion policy. Direct indicates training solely on the finetuning dataset  $\mathcal{D}_{\text{new}}$ , whereas P+F indicates pretraining on the original domain expert dataset  $\mathcal{D}$  followed by finetuning on  $\mathcal{D}_{\text{new}}$ .

## V. EXPERIMENTS

### A. Robot Setup

There are two robots involved in our tasks: a customized robot, and a Franka Emika Panda robot.

Our customized robot features a height-adjustable rail, two 7-degree-of-freedom Realman arms (each with a 2-degree-of-freedom gripper), and an Intel RealSense D435 camera mounted on the rail (Figure 4a). The rail joint value indicates the distance to the top in centimeters. In practice, we use the camera and one of the two arms mounted on the rail. The robot is controlled with PD control joint position scheme, and the action for arm is delta position, while the action for gripper is absolute position.

The Franka Emika Panda robot is a 7-degree-of-freedom arm with a 2-degree-of-freedom gripper. It is controlled in the same way as our customized robot. For our tasks, the Panda is fixed on a tabletop and used only in simulation (Figure 4b).

### B. Task Descriptions

We evaluate the baselines and our approach on six tasks in the sim-to-sim transfer experiments, three of which are also used in the sim-to-real transfer experiments. The details of these tasks are described below:

- (i) **Cabinet Open.** The task features a cabinet with a rail-mounted sliding drawer equipped with a front handle. Beginning from the closed position, the robot arm must reach the handle, secure it with the gripper, and pull the drawer open to about 50% of its full rail length. The cabinet is randomly initialized within a  $20 \times 20 \times 10 \text{ cm}^3$  space (along the  $x$ ,  $y$ , and  $z$  axes) in simulation, and within a  $15 \times 10 \text{ cm}^2$  area (in the  $x-y$  plane) in the real world.
- (ii) **Push Cube.** The task involves manipulating a cube placed on the table surface using the robot arm. The arm must push the cube with its gripper until it reaches a specified target position on the table, which is designed as a circle with its center 20 cm away from the cube and a radius of 10 cm. The cube is randomly initialized

within a  $20 \times 20 \times 10 \text{ cm}^3$  space (along the  $x$ ,  $y$ , and  $z$  axes) in simulation, and within a  $10 \times 10 \text{ cm}^2$  area (in the  $x-y$  plane) in the real world.

- (iii) **Pick Cube.** The task requires the robot arm to grasp a cube placed on the tabletop and lift it to a specified target position, which is designed to be 15 cm above the cube. The cube is randomly initialized within a  $20 \times 20 \times 10 \text{ cm}^3$  space (along the  $x$ ,  $y$ , and  $z$  axes) in simulation, and within a  $10 \times 10 \text{ cm}^2$  area (in the  $x-y$  plane) in the real world.
- (iv) **Peg Insertion.** The task requires the robot arm to grasp a peg with its gripper and insert it into a narrow hole of matching size. This task demands highly precise manipulation, and many offline imitation learning methods struggle with it due to bias accumulation. The peg is randomly initialized within a  $20 \times 30 \text{ cm}^2$  area (along the  $x$  and  $y$  axes), and the box is initialized within a  $10 \times 20 \text{ cm}^2$  area in simulation. This task is evaluated only in simulation.
- (v) **Roll Ball.** The task involves manipulating a ball placed on the table surface using the robot arm. The arm must push the ball with its gripper towards a randomly chosen target region on the table, defined as a circle located several decimeters away with a radius of 10 cm. The ball is randomly initialized within a  $30 \times 20 \text{ cm}^2$  area (along the  $x$  and  $y$  axes). This task is evaluated only in simulation.
- (vi) **Lift Peg Upright.** The task requires the robot arm to grasp a peg with its gripper and lift to any upright position on the table. The peg is randomly initialized within a  $40 \times 40 \text{ cm}^2$  area (along the  $x$  and  $y$  axes) in simulation. This task is evaluated only in simulation.

The first three tasks are performed with our customized robot, whereas the latter three use a Franka Panda arm. Illustrations of the tasks are shown in Figure 3.

### C. Baselines

For baselines, we evaluate two standard offline imitation learning methods, including behavioral cloning (BC) with an encoder and a Gaussian policy, and diffusion policy

(DP) [7], to highlight the effectiveness of our online imitation pretraining approach. Each baseline is trained under two settings:

- (i) **Direct**: training solely on the finetuning expert dataset  $\mathcal{D}_{\text{new}}$  from the new domain.
- (ii) **Pretrain + Finetune (P+F)**: first training on the expert dataset  $\mathcal{D}$  from the original domain, then finetuning on  $\mathcal{D}_{\text{new}}$  from the new domain.

#### D. Sim-to-Sim Transfer Results

We study *sim-to-sim* domain adaptation in robot arm manipulation tasks in ManiSkill3 simulation environments [34], considering two types of domain gaps:

- (i) **Biased pose estimations**: a bias is introduced into the object poses of the new domain to simulate imperfect pose information.
- (ii) **Robot Kinematics Gap**: the robot arm’s rail is shifted to a new location along with biased pose estimations, distinct from that in the pretrained environment.

Both types of gaps capture realistic challenges: pose estimation is often subject to noise, and the actual height of a robot may not perfectly align with its simulated counterpart. The gaps are illustrated in Figure 5 and Table II. Since the Franka Panda robot does not use a rail, we conduct experiments only with biased pose estimation for tasks involving this robot. The number of expert trajectories used for pretraining and finetuning is detailed in Table III. For expert data sampling in both pretraining and finetuning phases, we use a trained TD-MPC2 [10] for the Pick Cube task, PPO [9] for the Roll Ball task, and SAC [8] for all remaining tasks.

We evaluate both the baselines and our method over 100 episodes, reporting the success rates in Table I. Results demonstrate that in all of the 9 different settings across the 6 sim-to-sim tasks, our CDRED-WM method can achieve the best performance when comparing with baseline methods with offline imitation pretraining. In 5 of the 9 task settings, our CDRED-WM method can achieve at least 15% better results than the second best methods, among which Push Cube Biased State, Peg Insertion and Lift Peg Upright settings experience more than 30% performance boost. These findings highlight the robustness and strong generalization of our method with online imitation pretraining and offline imitation finetuning in domain transfer tasks.

#### E. Sim-to-Real Transfer Results

We evaluate the following tasks in the sim-to-real setting: Cabinet Open, Push Cube, and Pick Cube. For each task, we

Tasks	Pose Bias (cm)	Kinematics Gap
Cabinet Open	(2, 2, 2)	5 cm ↓
Push Cube	(2, 2, 1)	5 cm ↓
Pick Cube	(2, 2, 1)	2 cm ↑
Peg Insertion	(1, 1, 1)	-
Roll Ball	(2, 2, 1)	-
Lift Peg Upright	(2, 2, 2)	-

TABLE II: Sim-to-Sim domain gaps.

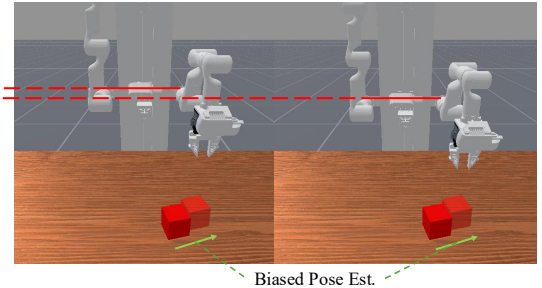


Fig. 5: **Domain Gap in Sim-to-Sim Domain Transfer.** We illustrate the two types of domain gaps considered in our sim-to-sim transfer experiments. During finetuning in the target domain, the policy must adapt to either biased pose estimation or a shifted rail position.

use the simulation-pretrained CDRED world model as base model (same pretrained model as in sim-to-sim settings) and collect 30 real-world expert trajectories for finetuning. To obtain these trajectories, we first pretrain a CDRED world model in simulation and then incorporate human corrections into the direct rollouts of the pretrained model during real-world execution. We evaluate both the baselines and our method over 10 episodes, reporting the success rates in Table IV.

Results demonstrate that with same amount of real-world expert trajectories, our CDRED-WM method performs much better than the baseline methods on the Cabinet Open task. For the Push Cube and Pick Cube tasks, our CDRED method significantly outperforms the BC-based baselines, while slightly outperforms the DP-based baselines. Overall, CDRED-WM method can achieve more stable and better results when comparing with baseline methods on the three tasks, which shows its strong potential in sim-to-real.

#### F. Benefits of Online Imitation Pretraining

a) **Better Coverage for Pretraining:** Offline imitation learning approaches such as behavioral cloning (BC) [35] and diffusion policy [7] fit only the distribution of the offline expert dataset. When the expert dataset is small and lacks sufficient coverage, the resulting pretrained policy becomes narrowly distributed and may suffer from distributional collapse during finetuning. Incorporating online reward-free interactions during pretraining expands coverage of the state space, which improves generalization and mitigates bias accumulation (a key factor impacting the performance of

Dataset	$\mathcal{D}$		
	Original	Biased Pose	Kinematics Gap
Domain			
Cabinet Open	200	100	100
Push Cube	200	30	50
Pick Cube	400	100	100
Peg Insertion	400	100	-
Roll Ball	400	100	-
Lift Peg Upright	100	10	-

TABLE III: Number of expert trajectories used in sim-to-sim tasks.

Tasks	BC (Direct)	BC (P+F)	DP (Direct)	DP (P+F)	CDRED-WM (Ours)
Cabinet Open	6/10	1/10	4/10	3/10	<b>9/10</b>
Push Cube	2/10	5/10	<b>8/10</b>	7/10	<b>8/10</b>
Pick Cube	0/10	7/10	7/10	<b>10/10</b>	<b>10/10</b>
Total	8/30	13/30	19/30	20/30	<b>27/30</b>

TABLE IV: **Sim-to-Real Transfer Results.** We evaluate our approach against baseline methods on three sim-to-real transfer tasks using our customized robot. Each task is assessed over 10 trajectories, and the success rate is reported. Our method achieves the highest success rate compared to existing offline imitation learning approaches.

offline IL in the Peg Insertion and Roll Ball tasks, as shown in Table I). Figure 6 compares the coverage of the offline expert dataset with that of the online exploration data, illustrating how online interactions substantially broaden the explored state space.

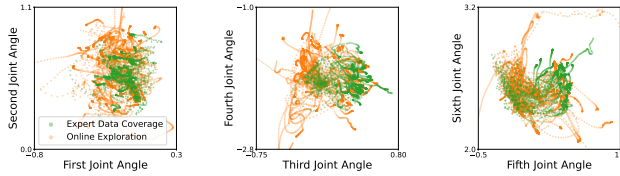


Fig. 6: **Data Coverage.** Visualization of state-space coverage from the expert dataset and online exploration using CDRED-WM in the Peg Insertion task, shown for six joint angles of the robot arm. The results indicate that online exploration effectively provides additional coverage in regions of the state space not represented in the expert dataset.

*b) Less Performance Degradation after Finetuning:*

Compared to offline pretraining with DP or BC, our online imitation learning approach exhibits less performance degradation under supervised finetuning domain transfer. Results in Table V show that BC and diffusion policy suffer significant drops in success rate after finetuning with limited expert data from the new domain, whereas our approach largely preserves performance. A possible explanation is that online imitation pretraining, through active exploration, achieves broader coverage of the state-action space rather than narrowly fitting the offline expert dataset, thereby improving robustness to distribution shifts in domain transfer. This issue is further amplified by the relatively small size of the pretraining expert dataset, underscoring that our online imitation pretraining approach is more robust in limited data regimes. Prior work on offline-to-online RL [36], [37] has similarly observed that directly finetuning offline-pretrained policies can lead to performance degradation and distributional collapse when encountering OOD transitions, due to their limited policy support. This analogy suggests that online pretraining provides a robustness advantage over purely offline pretraining in imitation learning as well.

*c) Stronger Out-of-distribution Generalization Ability:*

Additionally, we evaluate the out-of-distribution generalization ability of our online imitation pretraining approach. In the domain transfer phase, expert data from the new domain is collected from a narrow set of initial states, while evaluation is performed on unseen initializations. We

Domain	BC	DP	CDRED-WM (Ours)
Original	90%	86%	96%
New (Finetuned)	37%	62%	96%
Degradation	-53%	-24%	-0%

TABLE V: **Performance Degradation after Supervised Finetuning.** We analyze the performance degradation after finetuning on a new domain with incorrect state estimation gap compared to the performance on the original domain on Push Cube task. Results show that our online imitation pretraining approach suffers less after finetuning on a new domain compared to existing offline imitation learning approaches.

Setting	BC	DP	CDRED-WM (Ours)
I.D.	51%	36%	66%
O.O.D.	28%	8%	62%
Degradation	-23%	-28%	-4%

TABLE VI: **Generalization to Unseen Initializations.** We evaluate success rates over 100 trajectories by deploying the model on initializations not included in the finetuning dataset. The results show that our method exhibits less performance degradation, indicating stronger out-of-distribution generalization. “I.D.” denotes in-distribution settings, while “O.O.D.” denotes out-of-distribution settings.

study this setting using the Cabinet Open task, where the deployment initialization of the cabinet is shifted by 20cm, which is completely outside the range used for finetuning trajectory sampling. As shown in Table VI, our method achieves stronger performance on these unseen initializations compared to offline imitation pretraining baselines.

#### G. Ablation Studies

We conduct the ablation study on the number of expert trajectories required during finetuning for our approach in simulation domain transfer. We conduct this evaluation on Cabinet Open task. Results in Table VII show that our approach can still achieve 50% success rate with only 20 expert trajectories from the new domain with biased state estimation.

#### H. Hyperparameter Settings

During finetuning, we optimize the encoder and policy using the supervised finetuning objective with a learning rate of  $1 \times 10^{-5}$  and a weight decay of  $1 \times 10^{-4}$ . We use a batch

Trajectory Number	Success Rate
100	62%
50	56%
20	50%
10	42%

**TABLE VII: Ablation Study on Finetuning Trajectory Number.** We perform an ablation over the number of finetuning trajectories (100, 50, 20, and 10) and report success rates on 100 evaluation trajectories.

size of 256 and a horizon of 3. Pretraining hyperparameters are the same as in the original CDRED paper [11].

## VI. CONCLUSIONS

In this paper, we propose a sim-to-real framework based on world models for settings with no reward signals and only limited expert data in both simulation and the real world. Our approach employs a CDRED reward model to generate surrogate rewards by discriminating expert from behavioral data, thereby facilitating world model training. The pretrained model is then finetuned on a few-shot real-world expert dataset. We evaluate our method on six sim-to-sim manipulation transfer tasks with two manually designed domain gaps, as well as three sim-to-real manipulation tasks on real robots. Experimental results demonstrate that our approach improves success rates by at least 31.7% in sim-to-sim transfer and 23.3% in sim-to-real transfer compared to state-of-the-art offline imitation learning baselines.

## REFERENCES

- [1] Y. Feng, N. Hansen, Z. Xiong, C. Rajagopalan, and X. Wang, “Finetuning offline world models in the real world,” *arXiv preprint arXiv:2310.16029*, 2023.
- [2] T.-D. Do, N. Gireesh, J. Wang, and H. Wang, “Watch less, feel more: Sim-to-real rl for generalizable articulated object manipulation via motion adaptation and impedance control,” *arXiv preprint arXiv:2502.14457*, 2025.
- [3] Z. Ding, Y.-Y. Tsai, W. W. Lee, and B. Huang, “Sim-to-real transfer for robotic manipulation with tactile sensory,” in *2021 IEEE/RSJ International Conference on Intelligent Robots and Systems (IROS)*. IEEE, 2021, pp. 6778–6785.
- [4] T. Lin, K. Sachdev, L. Fan, J. Malik, and Y. Zhu, “Sim-to-real reinforcement learning for vision-based dexterous manipulation on humanoids,” *arXiv:2502.20396*, 2025.
- [5] W. Cai, J. Peng, Y. Yang, Y. Zhang, M. Wei, H. Wang, Y. Chen, T. Wang, and J. Pang, “Navdp: Learning sim-to-real navigation diffusion policy with privileged information guidance,” *arXiv preprint arXiv:2505.08712*, 2025.
- [6] A. Maddukuri, Z. Jiang, L. Y. Chen, S. Nasiriany, Y. Xie, Y. Fang, W. Huang, Z. Wang, Z. Xu, N. Chernyadev, *et al.*, “Sim-and-real co-training: A simple recipe for vision-based robotic manipulation,” *arXiv preprint arXiv:2503.24361*, 2025.
- [7] C. Chi, S. Feng, Y. Du, Z. Xu, E. Cousineau, B. Burchfiel, and S. Song, “Diffusion policy: Visuomotor policy learning via action diffusion,” in *Proceedings of Robotics: Science and Systems (RSS)*, 2023.
- [8] T. Haarnoja, A. Zhou, P. Abbeel, and S. Levine, “Soft actor-critic: Off-policy maximum entropy deep reinforcement learning with a stochastic actor,” in *International conference on machine learning*. Pmlr, 2018, pp. 1861–1870.
- [9] J. Schulman, F. Wolski, P. Dhariwal, A. Radford, and O. Klimov, “Proximal policy optimization algorithms,” *arXiv preprint arXiv:1707.06347*, 2017.
- [10] N. Hansen, H. Su, and X. Wang, “Td-mpc2: Scalable, robust world models for continuous control,” 2024.
- [11] S. Li, Z. Huang, and H. Su, “Coupled distributional random expert distillation for world model online imitation learning,” *arXiv preprint arXiv:2505.02228*, 2025.
- [12] J. Ho and S. Ermon, “Generative adversarial imitation learning,” in *Neural Information Processing Systems*, 2016. [Online]. Available: <https://api.semanticscholar.org/CorpusID:16153365>
- [13] D. Garg, S. Chakraborty, C. Cundy, J. Song, and S. Ermon, “Iq-learn: Inverse soft-q learning for imitation,” in *Thirty-Fifth Conference on Neural Information Processing Systems*, 2021.
- [14] H. Xiao, M. Herman, J. Wagner, S. Ziesche, J. Etesami, and T. H. Linh, “Wasserstein adversarial imitation learning,” 2019.
- [15] F. Al-Hafez, D. Tateo, O. Arenz, G. Zhao, and J. Peters, “Ls-iq: Implicit reward regularization for inverse reinforcement learning,” in *Eleventh International Conference on Learning Representations (ICLR)*, 2023.
- [16] S. Reddy, A. D. Dragan, and S. Levine, “Sqil: Imitation learning via regularized behavioral cloning,” *ArXiv*, vol. abs/1905.11108, 2019.
- [17] J. Ren, G. Swamy, Z. S. Wu, J. A. Bagnell, and S. Choudhury, “Hybrid inverse reinforcement learning,” 2024.
- [18] Z.-H. Yin, W. Ye, Q. Chen, and Y. Gao, “Planning for sample efficient imitation learning,” in *Neural Information Processing Systems*, 2022.
- [19] S. Li, Z. Huang, and H. Su, “Reward-free world models for online imitation learning,” in *International Conference on Machine Learning (ICML)*, 2025.
- [20] H. Niu, J. Hu, G. Zhou, and X. Zhan, “A comprehensive survey of cross-domain policy transfer for embodied agents,” in *Proceedings of the Thirty-Third International Joint Conference on Artificial Intelligence*, 2024, pp. 819–8206.
- [21] M. Torne, A. Simeonov, Z. Li, A. Chan, T. Chen, A. Gupta, and P. Agrawal, “Reconciling reality through simulation: A real-to-sim-to-real approach for robust manipulation,” *arXiv preprint arXiv:2403.03949*, 2024.
- [22] J. Matas, S. James, and A. J. Davison, “Sim-to-real reinforcement learning for deformable object manipulation,” in *Proceedings of The 2nd Conference on Robot Learning*, ser. Proceedings of Machine Learning Research, A. Billard, A. Dragan, J. Peters, and J. Morimoto, Eds., vol. 87. PMLR, 29–31 Oct 2018, pp. 734–743.
- [23] X. Zhang, C. Wang, L. Sun, Z. Wu, X. Zhu, and M. Tomizuka, “Efficient sim-to-real transfer of contact-rich manipulation skills with online admittance residual learning,” in *Conference on Robot Learning*. PMLR, 2023, pp. 1621–1639.
- [24] S. Patel, X. Yin, W. Huang, S. Garg, H. Nayyeri, L. Fei-Fei, S. Lazebnik, and Y. Li, “A real-to-sim-to-real approach to robotic manipulation with vlm-generated iterative keypoint rewards,” *arXiv preprint arXiv:2502.08643*, 2025.
- [25] W. Wan, J. Fu, X. Yuan, Y. Zhu, and H. Su, “Lodestar: Long-horizon dexterity via synthetic data augmentation from human demonstrations,” *arXiv preprint arXiv:2508.17547*, 2025.
- [26] D. Hafner, T. Lillicrap, I. Fischer, R. Villegas, D. Ha, H. Lee, and J. Davidson, “Learning latent dynamics for planning from pixels,” in *International conference on machine learning*. PMLR, 2019, pp. 2555–2565.
- [27] D. Hafner, T. Lillicrap, J. Ba, and M. Norouzi, “Dream to control: Learning behaviors by latent imagination,” *arXiv preprint arXiv:1912.01603*, 2019.
- [28] N. Hansen, X. Wang, and H. Su, “Temporal difference learning for model predictive control,” *arXiv preprint arXiv:2203.04955*, 2022.
- [29] D. Hafner, J. Pasukonis, J. Ba, and T. Lillicrap, “Mastering diverse domains through world models,” *arXiv preprint arXiv:2301.04104*, 2023.
- [30] Z.-H. Yin, W. Ye, Q. Chen, and Y. Gao, “Planning for sample efficient imitation learning,” *Advances in Neural Information Processing Systems*, vol. 35, pp. 2577–2589, 2022.
- [31] Y. Burda, H. Edwards, A. Storkey, and O. Klimov, “Exploration by random network distillation,” *arXiv preprint arXiv:1810.12894*, 2018.
- [32] N. Ravi, V. Gabeur, Y.-T. Hu, R. Hu, C. Ryali, T. Ma, H. Khedr, R. Rädlé, C. Rolland, L. Gustafson, *et al.*, “Sam 2: Segment anything in images and videos,” *arXiv preprint arXiv:2408.00714*, 2024.
- [33] B. Wen, W. Yang, J. Kautz, and S. Birchfield, “Foundationpose: Unified 6d pose estimation and tracking of novel objects,” in *Proceedings of the IEEE/CVF Conference on Computer Vision and Pattern Recognition*, 2024, pp. 17868–17879.
- [34] S. Tao, F. Xiang, A. Shukla, Y. Qin, X. Hinrichsen, X. Yuan, C. Bao, X. Lin, Y. Liu, T.-K. Chan, *et al.*, “Maniskill3: Gpu parallelized robot simulation and rendering for generalizable embodied ai,” in *7th Robot Learning Workshop: Towards Robots with Human-Level Abilities*.

- [35] M. Bain and C. Sammut, “A framework for behavioural cloning.” in *Machine intelligence 15*, 1995, pp. 103–129.
- [36] Z. Zhou, A. Peng, Q. Li, S. Levine, and A. Kumar, “Efficient online reinforcement learning fine-tuning need not retain offline data,” *arXiv preprint arXiv:2412.07762*, 2024.
- [37] Y. Shin, J. Kim, W. Jung, S. Hong, D. Yoon, Y. Jang, G. Kim, J. Chae, Y. Sung, K. Lee, *et al.*, “Online pre-training for offline-to-online reinforcement learning,” *arXiv preprint arXiv:2507.08387*, 2025.